



# Characterization of a *Salmonella* Transcription Factor-DNA Complex and Identification of the Inducer by Native Mass Spectrometry

Blake E. Szkoda<sup>1,2†</sup>, Angela Di Capua<sup>1,3†</sup>, Joy Shaffer<sup>1‡</sup>, Edward J. Behrman<sup>1</sup>, Vicki H. Wysocki<sup>1,2,3,4\*</sup> and Venkat Gopalan<sup>1,2,4\*</sup>

**1** - Department of Chemistry and Biochemistry, The Ohio State University, Columbus, OH 43210, USA

**2** - The Ohio State Biochemistry Program, The Ohio State University, Columbus, OH 43210, USA

**3** - Resource for Native Mass Spectrometry-Guided Structural Biology, The Ohio State University, Columbus, OH 43210, USA

**4** - Center for RNA Biology, The Ohio State University, Columbus, OH 43210, USA

**Correspondence to Vicki H. Wysocki and Venkat Gopalan:** Department of Chemistry and Biochemistry, The Ohio State University, Columbus, OH 43210, USA. [wysocki.11@osu.edu](mailto:wysocki.11@osu.edu) (V.H. Wysocki), [gopalan.5@osu.edu](mailto:gopalan.5@osu.edu) (V. Gopalan)

<https://doi.org/10.1016/j.jmb.2022.167480>

Edited by Patrick Griffin

## Abstract

FraR, a transcriptional repressor, was postulated to regulate the metabolism of the Amadori compound fructose-asparagine (F-Asn) in the foodborne pathogen *Salmonella enterica*. Here, the DNA- and inducer-binding affinities and stoichiometries of FraR were determined and cross-validated by electrophoretic mobility-shift assays (EMSAs) and online buffer exchange coupled to native mass spectrometry (OBE-nMS). We demonstrate the utility of OBE-nMS to characterize protein and protein-DNA complexes that are not amenable to offline exchange into volatile buffers. OBE-nMS complemented EMSAs by revealing that FraR binds to the operator DNA as a dimer and by establishing 6-phosphofructose-aspartate as the inducer that weakens DNA binding by FraR. These results provide insights into how FraR regulates the expression of F-Asn-catabolizing enzymes and add to our understanding of the intricate bacterial circuitry that dictates utilization of diverse nutrients.

© 2022 Elsevier Ltd. All rights reserved.

## Introduction

*Salmonella enterica* (*Salmonella*) can utilize the naturally occurring Amadori product fructose-asparagine (F-Asn) as a source of carbon and nitrogen to support its growth.<sup>1</sup> The ability of *Salmonella* to convert F-Asn into glucose-6-phosphate and L-aspartate depends on the *fra* locus, which consists of five genes: *fraR*, *fraB*, *fraD*, *fraA*, and *fraE* (Figure 1(a)).<sup>1,2</sup> The regulation of *fra* gene expression by FraR, a putative transcriptional repressor, is not understood, a gap that we address here.

Qualitative and quantitative aspects of DNA-protein complexes have been studied by several

methods including electrophoretic mobility-shift assays (EMSAs), isothermal titration calorimetry (ITC), and surface plasmon resonance (SPR).<sup>3</sup> In addition to technical caveats associated with each method, attributes such as the stoichiometry of the DNA-protein complex, especially in the presence of small-molecule inducers that serve as on/off switches *in vivo*, still require confirmation by other approaches. In this regard, insights on protein-protein, protein-ligand, and protein-nucleic acid interactions have been gained from native mass spectrometry (nMS), a powerful analytical tool that allows study of macromolecular complexes in the gas phase where proteins remain folded and non-covalent interactions can be preserved.<sup>4,5</sup>

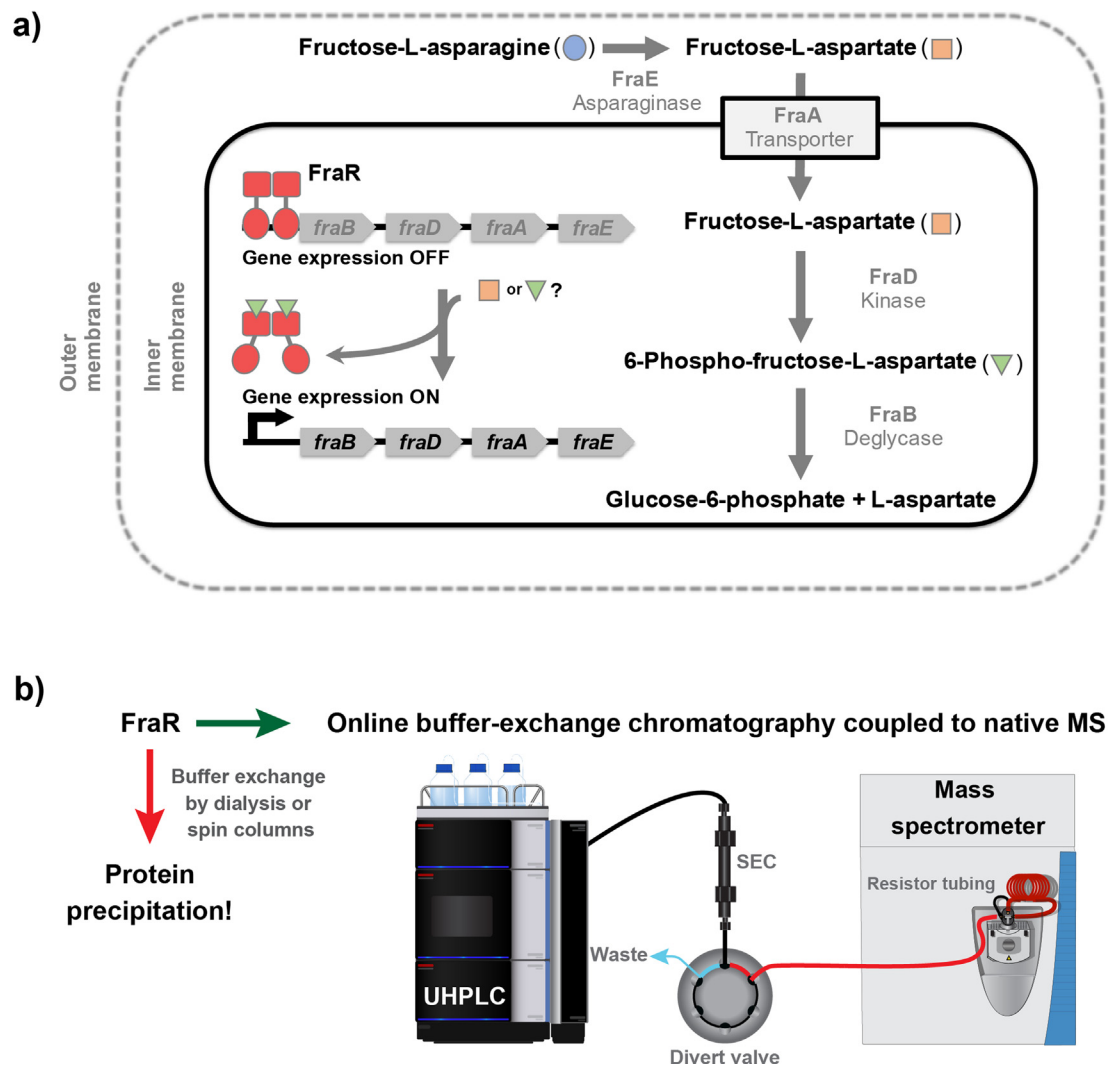


**Figure 1.** Fructose-asparagine (F-Asn) utilization in *Salmonella* and online buffer exchange coupled to native mass spectrometry (OBE-nMS). a) *Salmonella* uses a deglycase (FraB), kinase (FraD), and asparaginase (FraE) for F-Asn catabolism; FraA and FraR encode a putative transporter and transcriptional repressor, respectively. b) Schematic of the OBE-nMS system. Samples in suitable buffers are injected onto a size-exclusion/desalting column to separate biomolecules (elution at 0.6 min) from non-volatile salts (elution at 0.9 min; also, see Figure S13). Samples eluted in 200 mM ammonium acetate (mobile phase) are directed to the MS, while the non-volatile salts in the initial sample are diverted to waste. Figure in (b) was adapted from ref. 19. Copyright 2021 American Chemical Society.

Moreover, structural information such as stoichiometry, connectivity, and conformational changes can be obtained by coupling nMS to ion mobility, where species are separated based on their size and shape.<sup>6</sup> Likewise, nMS together with collision-induced dissociation and surface-induced dissociation can be used to elucidate protein stability and subcomplex connectivity. Furthermore, UV photodissociation and electron-based techniques such as electron capture dissociation and electron transfer dissociation, can furnish covalent fragmentation information that in turn is useful for mapping ligand binding sites and conformational changes.<sup>7,8</sup>

Despite the important advances fostered by nMS, there are some limitations. First, samples are usually analyzed in the nanomolar and micromolar concentration range thus limiting the scope of biological assemblies that can be investigated. Second, aggregation or precipitation under nMS conditions can remove some species from examination and affect spectral quality and accuracy. Third, in a typical nMS workflow, biological samples are buffer-exchanged into a solution of a volatile salt (e.g., ammonium acetate) prior to nMS analysis. The use of a volatile electrolyte at the physiological pH and ionic

strength allows for transfer of biomolecules from solution to the gas phase without perturbing protein-binding interactions. Obtaining well-resolved mass spectral data, however, occasionally entails applying additional energy in the form of in-source trapping/in-source clean-up by heat and/or collisions with background gas.<sup>9,10</sup> Using such harsh conditions to obtain well-resolved peaks is appropriate when *only* an accurate mass is desired. For structural information (e.g., by activation and dissociation after mass selection), however, it may be preferable to use solvent- and salt-adducted ions for preserving native-like structures,<sup>8</sup> a choice further supported by findings that in-source trapping can cause structural rearrangements.<sup>11</sup> Last, some molecular assemblies require the presence of inorganic salts and other components to maintain their inter-subunit interactions and stability. However, nMS studies performed by using non-volatile salts or mixtures of non-volatile and volatile electrolytes can result in broad spectral peaks,<sup>12,13</sup> due to salt adduction and poor desolvation. Although submicron tip emitters can minimize salt adducts for some samples analyzed directly from non-volatile buffer,<sup>14,16</sup> the use of small-tip emitters can also cause clogging and spray instability. Clearly, finding conditions that preserve the native features of biological assemblies while rendering them compatible for nMS can be difficult for some samples. Here, we provide one solution.

OBE-nMS is a technique that allows rapid buffer exchange of proteins from non-volatile to volatile buffers prior to direct electrospray of the exchanged sample into the mass spectrometer<sup>17</sup> OBE, which relies on HPLC and a “desalting” chromatographic column to separate and substitute non-volatile components with a volatile electrolyte as the mobile phase (Figure 1(b)), has been used to study individual recombinant proteins, protein-protein complexes, and overexpressed proteins in crude cell lysates.<sup>17–19</sup> Here, we combined fluorescence-based EMSAs and OBE-nMS to elucidate the DNA- and inducer-binding affinities and stoichiometries of *Salmonella* FraR, and expect this strategy to be broadly applicable for study of nucleoprotein complexes, even in cases (such as the one illustrated here) where the complex precipitates with off-line buffer exchange.

The *fra* locus includes the gene for FraR,<sup>1</sup> a member of the GntR transcription factor superfamily and the HutC subfamily.<sup>20</sup> FraR is postulated to bind to the *fraB* promoter (FBP)<sup>1</sup> and prevent transcription of the *fra* locus until its binding to an inducer (not yet identified) that causes de-repression and *fraB-DAE* gene expression (Figure 1(a)). A FraR homolog called FrIR regulates the metabolism of fructose-lysine (F-Lys), another Amadori product in *Escherichia coli*.<sup>21–23</sup> GntR members (like FraR and FrIR) typically contain a helix-turn-helix N-terminal DNA binding domain (DBD) and a variable

C-terminal inducer binding domain (IBD) that also facilitates dimerization.<sup>24</sup> Binding of an inducer to the IBD triggers a conformational change and weakens the affinity of the DBD for DNA as revealed by crystal structures of the HutC subfamily homolog *Bacillus subtilis* NagR, which regulates N-acetylglucosamine metabolism.<sup>24</sup> Here, we sought to better understand FraR, especially the location of its DNA-binding site in the *fra* locus, its stoichiometry  $\pm$  DNA, and the identity of its inducer metabolite.

### Identifying the DNA binding site and cellular inducer of *Salmonella* FraR

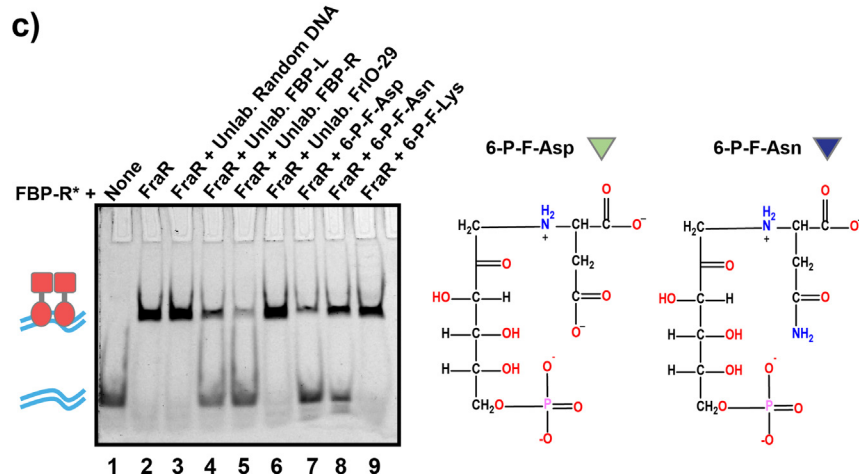
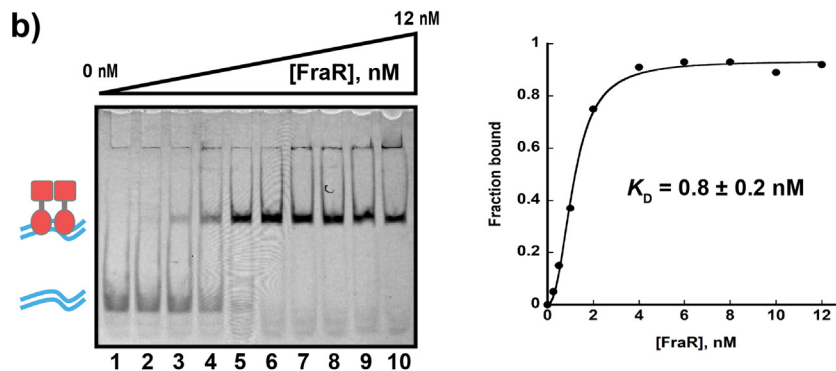
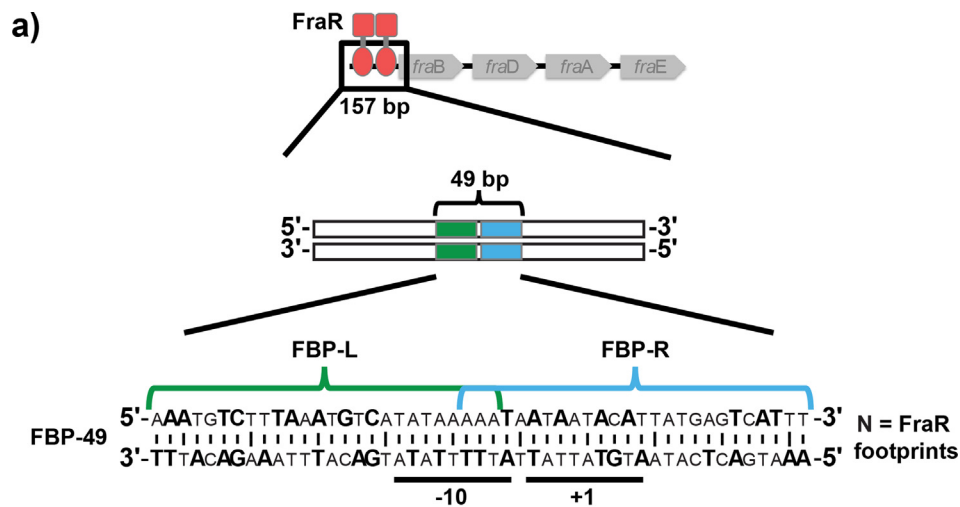
We obtained recombinant *Salmonella* FraR after its overexpression in *E. coli* as a fusion with maltose-binding protein and subsequent purification using immobilized metal affinity chromatography (Figure S1). To identify the minimal FraR binding site in the FBP, we used EMSAs to test the binding of FraR to a Cy5-labeled 157-bp DNA fragment (Table S1). This fragment represents –175 to –18 relative to the start codon of the *FraB* gene (where +1 refers to the “A” in the ATG start codon). After confirming that FraR bound this DNA, we used sequential deletions to pare down the FraR-binding site to a 49-bp region (FBP-49) that represents –93 to –44 in the upstream sequence (Figure 2(a), Figure S2(a)). Capillary electrophoresis-based DNase I footprinting experiments revealed the presence of two FraR binding sites within this 49-bp fragment and inspired our design of two minimal 26 bp DNAs that we termed FBP-R and FBP-L (Figure 2(a), Figure S2(a)).

The binding data from our EMSAs conducted with either FBP-R or FBP-L yielded dissociation constants ( $K_D$ ) of  $0.8 \pm 0.2$  nM or  $1.1 \pm 0.3$  nM, respectively (Figure 2(b), Figure S2(b), Figure S3). Based on these  $K_D$  values, we used 0.5 nM FBP-R or FBP-L and 2 nM FraR to achieve near-complete assembly and then sought to disrupt each DNA-protein complex with non-fluorescent DNAs or potential inducers (Figure 2(c), Figure S2(c)). Specificity of DNA binding by FraR is evident from our finding that dissociation of the FraR–FBP-R (or FraR–FBP-L) complex resulted *only* upon addition of competing non-fluorescent versions of FBP-L or FBP-R and *not* a 26-bp DNA with a random sequence but the same nucleotide composition as FBP-L and FBP-R (Figure 2(c), Figure S2(c)). Likewise, even a minimal 29-bp DNA corresponding to the binding site of *E. coli* FrIR (a FraR homolog) was unable to outcompete FBP-L or FBP-R bound to FraR (Figure 2(c), Figure S2(c)).

Our next goal was to establish the identity of the inducer that derepresses FraR. Given the F-Asn catabolic pathway (Figure 1(a)) and knowledge of NagR and FrIR inducers, the likely candidates

were F-Asp or 6-P-F-Asp as both are found in the cytoplasm and are downstream metabolites of F-Asn.<sup>23,24</sup> To ascertain specificity of ligand binding, we synthesized in-house a panel of Amadori metabolites<sup>1,25,26</sup> (all commercially unavailable), and report the first synthesis of 6-P-F-Lys starting with glucose-6-phosphate and  $\alpha$ -formyl-lysine (Figure S4 and Supplementary Text). Dissociation of the FBP-R–FraR or FBP-L–FraR was most effec-

tive with 6-P-F-Asp followed by 6-P-F-Asn (an Amadori derivative not reported in nature but synthesized here to test the essentiality of Asp in 6-P-F-Asp) and not at all by the  $\epsilon$ -conjugated 6-P-F-Lys, the postulated inducer of *E. coli* FrlR<sup>23</sup> (Figure 2(c), Figure S2(c)). Other Amadori compounds (e.g., F-Asp, F-Asn) did not cause dissociation of FBP-R–FraR (Figure S5). Further investigation revealed that titrating 6-P-F-Asp predictably



increased dissociation of the FraR–FBP–R complex (Figure S6).

### Characterization of the FraR–DNA complex using OBE–nMS

Despite the reproducible detection of FraR–FBP–R/FBP–L complexes by EMSAs and gaining insights into the identity of the inducer that acts to weaken FraR's affinity for DNA, we could not determine the stoichiometry of the complex. To obtain this information, we explored the use of nMS which has been used before for studying the interactions of transcription factors with DNA or inducers.<sup>10,27</sup> However, FraR precipitated upon dialysis into volatile ammonium acetate-based solutions regardless of pH or inclusion of various additives (e.g., detergents). Therefore, we directed our efforts to the use of OBE–nMS<sup>17</sup> for investigating FraR either free or bound to its DNA ligand ( $\pm$ inducer).

We first measured the molecular masses of FraR and the DNAs individually. OBE–nMS data for recombinant FraR resulted in an average molecular mass of  $54,407 \pm 1$  Da, validating a homodimeric state (Figure 3(a), Figure S7(a), Figure S8(a), Table S2) and consistent with the oligomeric state reported for some other members of the GntR family.<sup>20,23,24</sup> The observed molecular masses of  $15,931 \pm 1$  Da for FBP–L and  $15,932 \pm 1$  Da for FBP–R (Figures 3(b), S7(b), S8(b)–(c), Table S3) are in agreement with the expected masses. Next, we assembled FraR with either FBP–L or FBP–R and observed species with a molecular mass of  $70,340 \pm 1$  Da for (FraR)<sub>2</sub>–FBP–L and  $70,339 \pm 1$  Da for (FraR)<sub>2</sub>–FBP–R, consistent with binding of one FraR homodimer to one DNA copy (Figure 3(c), Figure S7(c), Figure S8(d)–(e), Table S2). Moreover, titration of FraR to a fixed concentration of FBP–R demonstrated a gradual increase in formation of the (FraR)<sub>2</sub>–FBP–R species with a small amount of (FraR)<sub>4</sub>–FBP–R

observed at excess FraR (Figure S9). In addition to providing insights into stoichiometry, these results helped assign identities to the species observed in the EMSAs: the fastest migrating band corresponds to the monomeric 26–bp FBP–R and the slower migrating band, which becomes more prominent with increasing [FraR], corresponds to (FraR)<sub>2</sub>–FBP–R (Figure 2(b)–(c)).

We then used OBE–nMS to evaluate the effect of different inducers on pre-formed FraR–FBP–R or FraR–FBP–L complexes. In the presence of 6–P–F–Asp, we did not observe any (FraR)<sub>2</sub>–FBP–R or (FraR)<sub>2</sub>–FBP–L complexes but instead found species corresponding to the (FraR–6–P–F–Asp)<sub>2</sub> complex and either free FBP–L or FBP–R (Figure 3(e), Figure S7(e), Figure S8(f)–(g)). We also probed 6–P–F–Asp binding directly to the protein and observed the same 2:2 stoichiometry (Figure 3(d), Figure S7(d), Figure S8(h), Table S2). Amadori compounds other than 6–P–F–Asp were also tested for binding to FraR but we did not detect any complex by OBE–nMS except with 6–P–F–Asn (Figure S10, Figure S11, Table S3), matching our EMSA results (Figure S5). 6–P–F–Asn also mirrored 6–P–F–Asp in its ability to bind FraR with the same 2:2 stoichiometry and cause FraR dimer dissociation (albeit not completely) from the bound DNA (Figure S11(b)).

To further characterize the (FraR–6–P–F–Asp)<sub>2</sub> complex, we employed OBE–nMS to investigate the apparent  $K_D$  for ligand binding, based on the assumption that the MS intensities reflect the same ratio of free:bound species that is present in solution. For this experiment, we fixed the [FraR, dimer] at 2  $\mu$ M, while varying [6–P–F–Asp] from 0 to 15  $\mu$ M. Interestingly, even at the lowest ligand concentrations that we tested, we did not observe any (FraR)<sub>2</sub> with only one 6–P–F–Asp bound (Figure 4, Figure S12). Using the Data Collector module available in Unidec software,<sup>28</sup> we



**Figure 2.** Mapping and characterizing the FraR binding sites in the *fraB* promoter (see Supplement for details on the footprinting procedure and Figure S2 for additional data). a) DNase I footprinting was used to localize a 49–bp region in the *fraB* promoter essential for binding two FraR homodimers. Based on the DNA–binding properties of other GntR members, whose binding sites are typically  $\sim 15$ – $18$  bp/dimer,<sup>20,23,24</sup> it seemed likely that this 49–bp segment might have two separate sites for FraR binding. To validate this idea, we constructed two DNAs termed FBP–L and FBP–R (26 bp each), both derived from the 49–bp DNA (denoted as FBP–49). b) Electrophoretic mobility–shift assays were performed to ascertain the binding affinity between FraR and Cy5–FBP–R (Cy5 denoted by \*, see Figure S2(b) for data on FBP–L). Varying amounts of FraR (0 to 12 nM, lanes 1 to 10) were incubated with 0.5 nM Cy5–FBP–R before these binding reactions were subjected to native PAGE [6% (w/v) acrylamide). The  $K_D$  value listed represents the mean  $\pm$  standard deviation calculated from three independent trials (see Figure S3 for all of the primary data). c) Dissociation of pre–formed FraR–Cy5–FBP–R complexes upon addition of competing unlabeled DNAs or Amadori compounds. After mixing Cy5–FBP–R (0.5 nM) and FraR (2 nM) to form a stable DNA–protein complex, the specificity of DNA binding or the inducer's identity, respectively, were determined by assessing the ability of competing non–fluorescent DNAs (added to a final concentration of 5 nM, lanes 3–6) or Amadori compounds (added to a final concentration of 2 mM, lanes 7–9) to cause dissociation of the Cy5–FBP–R–FraR complex. In panels b and c, the bands corresponding to Cy5–FBP–R (free DNA) and FraR–Cy5–FBP–R (bound DNA) are indicated by cartoon representations.

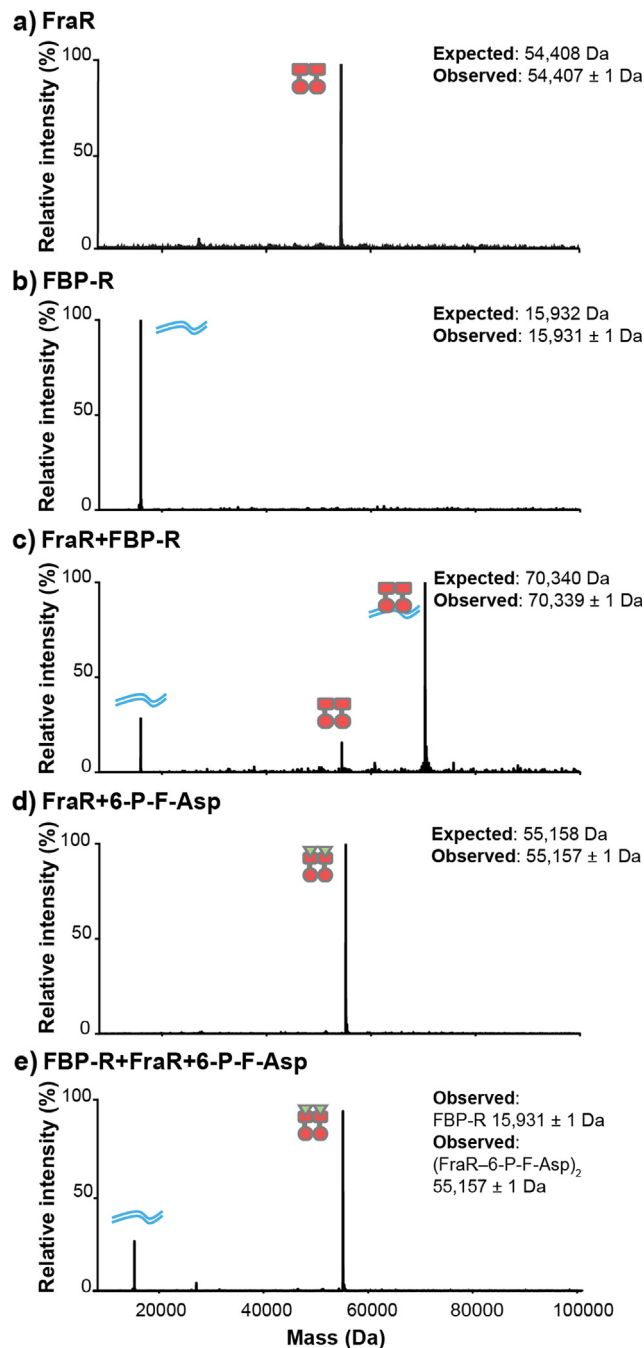


**Figure 3.** DNA- and inducer-binding stoichiometry of FraR (see Figure S7 for additional details and for data obtained with FBP-L). Dominant species in the deconvolved OBE-nMS spectra are indicated by cartoon representations. a) FraR<sub>2</sub>, b) FBP-R, c) FraR + FBP-R, d) FraR + 6-P-F-Asp, and e) FBP-R + FraR + 6-P-F-Asp. The expected and observed masses are listed (Table S2).

extracted the intensity values related to the deconvolved peaks and used GraphPad Prism to fit the data to a Hill equation since cooperativity was evident. Based on three replicates, we determined an apparent  $K_D$  of  $3.8 \pm 0.6 \mu\text{M}$  and  $n_H$  values of  $\sim 2$  for binding of 6-P-F-Asp to FraR (Figure 4, Figure S12). It is unclear if the apparent  $K_D$  might be influenced by the  $\sim 10$ – $15$ -fold dilution of samples undergoing OBE; whether the complex dissociates

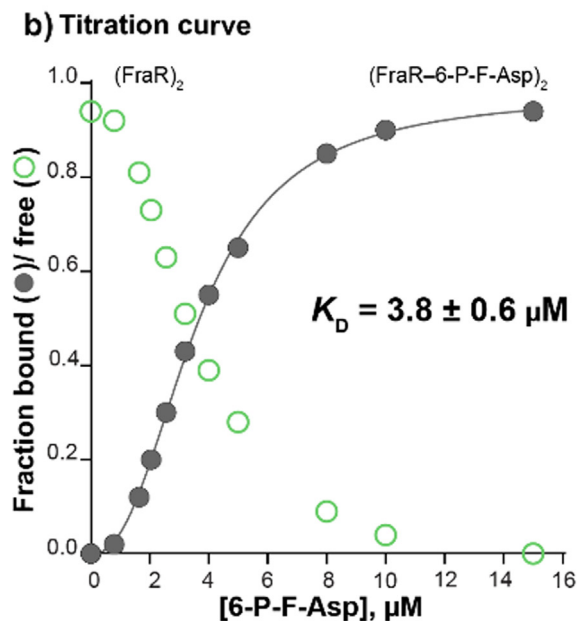
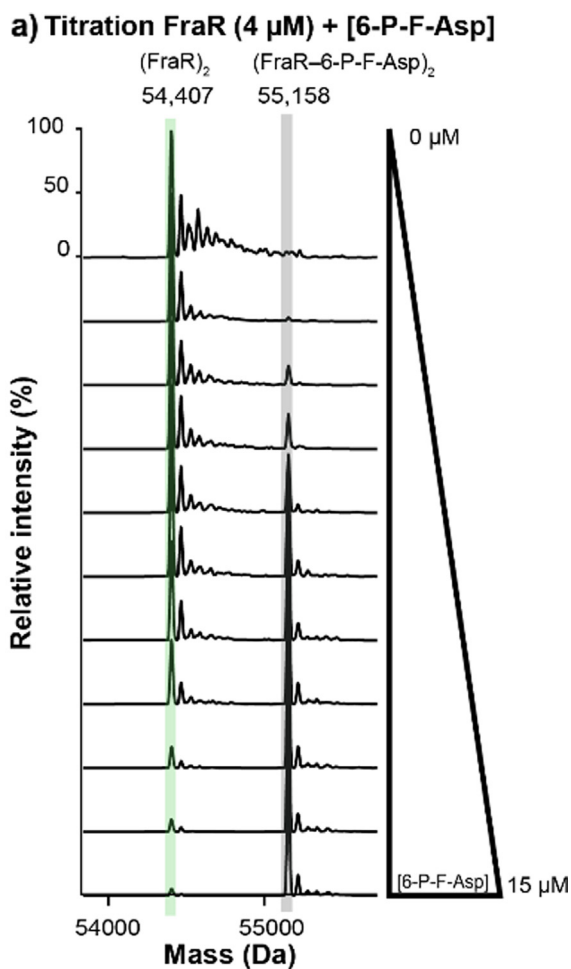
in the short ( $< 2$  min) time that it is on-column is uncertain.

## Concluding Remarks

Taken together, our findings from EMSA and OBE-nMS analyses permit a comparison of FraR attributes to other GntR family members and allow a few inferences with respect to how nutrient

availability is relayed to turn on bacterial catabolic pathways.

First, we demonstrated tight binding of FraR to two separate sites in the *fraB* promoter ( $K_D \sim 1$  nM each; Figure 2(b), Figure S2(b)). SPR



studies yielded  $K_D$  values of  $\sim 5$  nM and 20 pM, respectively, for the binding of FrlR to *friO* and NagR to *nagAB* operators.<sup>23,24</sup> The structural basis for such disparate DNA-binding affinities of FraR/FrlR compared to NagR merits study given that all of them are members of the HutC subfamily.

Second, the GntR transcription factors typically use an N-terminal helix-turn-helix motif to recognize the palindromic consensus sequence 5'-N<sub>y</sub>GTN<sub>x</sub>ACN<sub>y</sub>-3'.<sup>20</sup> In contrast to an earlier prediction of the FraR binding site,<sup>23</sup> our footprinting and binding studies suggest that FraR recognizes a sequence (5'-GTN<sub>2</sub>TTN<sub>2</sub>AT-3' in FBP-L and 5'-ATN<sub>2</sub>TAN<sub>2</sub>AC-3' in FBP-R) that deviates from the HutC consensus (5'-N<sub>y</sub>GTMTAKACN<sub>y</sub>-3'). Preliminary results from our mutagenesis studies (unpublished) support this non-consensus binding-site assignment and place FraR in the small number of GntR members that do *not* utilize the exact consensus sequence established for the HutC subfamily.

Third, our MS studies provide convincing evidence that each DNA binding site in the FBP is bound by a FraR dimer, echoing other GntR members (for an exception, see<sup>29</sup>). For example, the NagR homodimer, held together by tertiary contacts between the IBDs, uses the two DBDs for sequence-specific readout of two half-sites in the DNA palindrome. Moreover, bacterial two-hybrid assays, NMR, and size-exclusion chromatography experiments showed that the FrlR IBD is also capable of dimerization.<sup>23</sup>

Fourth, of the inducers that we tested by EMSA and OBE-nMS, only 6-P-F-Asp and its synthetic analog 6-P-F-Asn caused dissociation of the FraR-FBP-R/L complex; F-Asn, F-Asp, and 6-P-F-Lys were ineffective in this regard. The specific recognition of 6-P-F-Asp ( $\alpha$ -glycated) and not 6-P-F-Lys ( $\epsilon$ -glycated) mirrors the observation that the *S. enterica* FraB deglycase acts on 6-P-F-Asp and not 6-P-F-Lys. As pointed out earlier,<sup>23</sup> both the catabolic enzymes and the respective regulators are specific for either the  $\alpha$ - or  $\epsilon$ -glycated forms of the Amadori compounds. Moreover, the apparent  $K_D$  of 3.8  $\mu$ M for binding of 6-P-F-Asp to FraR

**Figure 4.** Determining the binding affinity of 6-P-F-Asp for FraR. FraR (4  $\mu$ M monomer) was titrated with different concentrations of 6-P-F-Asp before the samples were exchanged online into 200 mM ammonium acetate for OBE-nMS analysis. a) Deconvolved spectra of FraR in the presence of 6-P-F-Asp shows formation of (FraR-6-P-F-Asp)<sub>2</sub>. b) Determination of the apparent  $K_D$  for 6-P-F-Asp binding to FraR. Plot depicts the fraction of ligand bound-FraR dimer (●) that was fit to a quadratic Hill equation (see *Supplementary Information*). The corresponding decrease in free FraR dimer (○) is also shown. The apparent  $K_D$  value listed here represents the mean  $\pm$  standard deviation calculated from three independent trials (see Figure S12 for all of the primary data and the  $n_H$  values).

(established by OBE-nMS) suggests that de-repression is likely triggered even after modest uptake of F-Asn by *Salmonella*, indicating how bacteria have evolved sensitive sensors even for uncommon nutrients. Further support for this claim also stems from the cooperativity associated with binding of 6-P-F-Asp to FraR. Overall, these data identify 6-P-F-Asp as a tight-binding inducer of FraR, with its phosphate moiety being a necessary recognition determinant.

Finally, the use of a phosphorylated intermediate as the FraR inducer aligns with precedents established with other GntR members (e.g., NagR and N-acetylglucosamine-6-phosphate; DasR and glucosamine-6-phosphate; FrlR and 6-P-F-Lys).<sup>23,24,30</sup> Because phosphorylation is often the first step in sugar-utilization pathways, it is reasonable that these abundant and stable intermediates might be favored as inducers to regulate expression of the appropriate catabolic enzymes.

Our studies also motivate several questions. First, why are there two adjacent FraR binding sites in the *fraB* promoter? Are both important for regulation *in vivo*? Second, does FraR mirror NagR, which upon inducer binding promotes a displacement of its DBDs upwards by  $\sim 70$  Å in a “jumping-jack-like” motion and generates a conformation less competent for DNA binding? Such conformational dynamics of FraR  $\pm$  inducer warrant study. Finally, does binding of 6-P-F-Asp to FraR eliminate all DNA binding or dampen the specificity for its cognate DNA operator? Single-molecule studies that allow real-time observation of binding events and calculation of FraR dwell times while bound to specific versus non-specific DNA will be valuable.

In conclusion, our work highlights the complementarity of OBE-nMS and EMSA. OBE-nMS provided information on the stoichiometry of a DNA-protein complex not obtained by EMSA and allowed measurements of a protein that precipitated upon offline buffer exchange. Our results also provide insights into the regulation of Amadori metabolism in a clinically significant bacterial pathogen and uncover thematic parallels in control of gene expression during utilization of unrelated nutrients.

### CRedit authorship contribution statement

**Blake E. Szkoda:** Conceptualization, Methodology, Investigation, Writing – original draft. **Angela Di Capua:** Conceptualization, Methodology, Investigation, Writing – original draft. **Joy Shaffer:** Methodology, Resources. **Edward J. Behrman:** Conceptualization, Supervision, Funding acquisition. **Vicki H. Wysocki:** Conceptualization, Supervision, Project administration, Funding acquisition. **Venkat Gopalan:** Conceptualization, Supervision, Project administration, Funding acquisition.

### DECLARATION OF COMPETING INTEREST

The authors declare that they have no known competing financial interests or personal relationships that could have appeared to influence the work reported in this paper.

### Acknowledgements

We thank Andrew Norris, Zachary VanAernum, and Florian Busch for help with the OBE-nMS experiments, and Arpad Somogyi and the OSU Campus Chemical Instrument Center Mass Spectrometry and Proteomics Facility, for assistance with high-resolution MS studies. We are grateful to Christine Daugherty (OSUCC Genomics Shared Resource Center; P30CA016058) and Michael Zianni (Applied Biosystems) for their assistance with DNase I footprinting experiments. We thank Matthew Jajowka and Eleanor Bashian (OSU) for their contributions to initial FraR purification efforts. We thank Drs. Rosa Viner and Shane Bechler (Thermo Fisher Scientific, Sunnyvale, CA) for providing the prototype desalting cartridges. We thank Mark Foster, Sravya Kovvali, Edric Choi, and Richard Lease for valuable discussions, and Sophie Harvey and Stella Lai for input on figures. This work was supported by the NIH [P41-GM128577 (VHW), R01-AI116119 (EB, VG, and VHW; lead PI: Brian Ahmer), R01-AI140541 (BA and VG)], and a Camille and Henry Dreyfus Foundation Senior Scientist Mentor Program Award (EJB). BES was supported by NIH T32-GM086252 and a Presidential Fellowship from The OSU Graduate School. The 15T Bruker SolarixR FT-ICR instrument was purchased using funds from NIH S10 OD018507.

### Appendix A. Supplementary data

Supplementary data to this article can be found online at <https://doi.org/10.1016/j.jmb.2022.167480>.

Received 30 October 2021;

Accepted 31 January 2022;

Available online 14 February 2022

#### Keywords:

native mass spectrometry;  
*Salmonella* FraR;  
transcriptional regulation;  
fructose-asparagine utilization

† Equal contribution.

‡ Current address: Department of Chemistry & Biochemistry, University of Texas at Dallas, Richardson, TX 75080, USA.

### References

1. Ali, M.M., Newsom, D.L., González, J.F., Sabag-Daigle, A., Stahl, C., Steidley, B., et al., (2014). Fructose-asparagine is

- a primary nutrient during growth of *Salmonella* in the inflamed intestine. *PLoS Pathog.* **10**, e1004209
- Sabag-Daigle, A., Blunk, H.M., Sengupta, A., Wu, J., Bogard, A.J., Ali, M.M., et al., (2016). A metabolic intermediate of the fructose-asparagine utilization pathway inhibits growth of a *Salmonella fraB* mutant. *Sci. Rep.* **6**, 28117.
  - Dey, B., Thukral, S., Krishnan, S., Chakrobarty, M., Gupta, S., Manghani, C., et al., (2012). DNA-protein interactions: methods for detection and analysis. *Mol. Cell. Biochem.* **365**, 279–299.
  - Boeri Erba, E., Signor, L., Petosa, C., (2020). Exploring the structure and dynamics of macromolecular complexes by native mass spectrometry. *J. Proteomics* **222**, 103799
  - Tamara, S., den Boer, M.A., Heck, A.J.R., (2021). High-resolution native mass spectrometry. *Chem. Rev.*. <https://doi.org/10.1021/acs.chemrev.1c00212>.
  - Konijnenberg, A., Butterer, A., Sobott, F., (2013). Native ion mobility-mass spectrometry and related methods in structural biology. *BBA* **1834**, 1239–1256.
  - Snyder, D.T., Harvey, S.R., Wysocki, V.H., (2021). Surface-induced dissociation mass spectrometry as a structural biology tool. *Chem. Rev.*. <https://doi.org/10.1021/acs.chemrev.1c00309>.
  - Stiving, A.Q., VanAernum, Z.L., Busch, F., Harvey, S.R., Sarni, S.H., Wysocki, V.H., (2019). Surface-induced dissociation: an effective method for characterization of protein quaternary structure. *Anal. Chem.* **91**, 190–209.
  - Caldwell, B.J., Norris, A., Zakharova, E., Smith, C.E., Wheat, C.T., Choudhary, D., et al., (2021). Oligomeric complexes formed by Red $\beta$  single strand annealing protein in its different DNA bound states. *Nucleic Acids Res.* **49**, 3441–3460.
  - Shiu-Hin Chan, D., Seetoh, W.G., McConnell, B.N., Matak-Vinković, D., Thomas, S.E., Mendes, V., et al., (2017). Structural insights into the EthR-DNA interaction using native mass spectrometry. *Chem. Commun. (Camb.)* **53**, 3527–3530.
  - Harvey, S.R., VanAernum, Z.L., Wysocki, V.H., (2021). Surface-induced dissociation of anionic vs cationic native-like protein complexes. *J. Am. Chem. Soc.* **143**, 7698–7706.
  - Saikusa, K., Kato, D., Nagadoi, A., Kurumizaka, H., Akashi, S., (2020). Native mass spectrometry of protein and DNA complexes prepared in nonvolatile buffers. *J. Am. Soc. Mass Spectrom.* **31**, 711–718.
  - Ma, X., Lai, L.B., Lai, S.M., Tanimoto, A., Foster, M.P., Wysocki, V.H., et al., (2014). Uncovering the stoichiometry of *Pyrococcus furiosus* RNase P, a multi-subunit catalytic ribonucleoprotein complex, by surface-induced dissociation and ion mobility mass spectrometry. *Angew. Chem. Int. Ed. Engl.* **53**, 11483–11487.
  - Susa, A.C., Xia, Z., Williams, E.R., (2017). Native mass spectrometry from common buffers with salts that mimic the extracellular environment. *Angew. Chem. Int. Ed. Engl.* **56**, 7912–7915.
  - Xia, Z., DeGrandchamp, J.B., Williams, E.R., (2019). Native mass spectrometry beyond ammonium acetate: effects of nonvolatile salts on protein stability and structure. *Analyst.* **144**, 2565–2573.
  - Nguyen, G.T.H., Tran, T.N., Podgorski, M.N., Bell, S.G., Supuran, C.T., Donald, W.A., (2019). Nanoscale ion emitters in native mass spectrometry for measuring ligand-protein binding affinities. *ACS Cent. Sci.* **5**, 308–318.
  - VanAernum, Z.L., Busch, F., Jones, B.J., Jia, M., Chen, Z., Boyken, S.E., et al., (2020). Rapid online buffer exchange for screening of proteins, protein complexes and cell lysates by native mass spectrometry. *Nature Protoc.* **15**, 1132–1157.
  - Jia, M., Sen, S., Wachnowsky, C., Fidai, I., Cowan, J.A., Wysocki, V.H., (2020). Characterization of [2Fe-2S]-cluster-bridged protein complexes and reaction intermediates by use of native mass spectrometric methods. *Angew. Chem. Int. Ed. Engl.* **59**, 6724–6728.
  - Busch, F., VanAernum, Z.L., Lai, S.M., Gopalan, V., Wysocki, V.H., (2021). Analysis of tagged proteins using tandem affinity-buffer exchange chromatography online with native mass spectrometry. *Biochemistry* **60**, 1876–1884.
  - Suvorova, I.A., Korostelev, Y.D., Gelfand, M.S., (2015). GntR family of bacterial transcription factors and their DNA binding motifs: Structure, positioning and co-evolution. *PLoS ONE* **10**, e0132618
  - Deppe, V.M., Klatte, S., Bongaerts, J., Maurer, K.H., O'Connell, T., Meinhardt, F., (2011). Genetic control of Amadori product degradation in *Bacillus subtilis* via regulation of *friBONMD* expression by FriR. *Appl. Environ. Microbiol.* **77**, 2839–2846.
  - Wiame, E., Delpierre, G., Collard, F., Van Schaftingen, E., (2002). Identification of a pathway for the utilization of the Amadori product fructoselysine in *Escherichia coli*. *J. Biol. Chem.* **277**, 42523–42529.
  - Graf von Armansperg, B., Koller, F., Gericke, N., Hellwig, M., Jagtap, P.K.A., Heermann, R., et al., (2021). Transcriptional regulation of the N-fructoselysine metabolism in *Escherichia coli* by global and substrate-specific cues. *Mol. Microbiol.* **115**, 175–190.
  - Fillenberg, S.B., Grau, F.C., Seidel, G., Muller, Y.A., (2015). Structural insight into operator dre-sites recognition and effector binding in the GntR/HutC transcription regulator NagR. *Nucleic Acids Res.* **43**, 1283–1296.
  - Hansen, A.L., Behrman, E.J., (2016). Synthesis of 6-phosphofructose aspartic acid and some related Amadori compounds. *Carbohydr. Res.* **431**, 1–5.
  - Sengupta, A., Wu, J., Seffernick, J.T., Sabag-Daigle, A., Thomsen, N., Chen, T.H., et al., (2019). Integrated use of biochemical, native mass spectrometry, computational, and genome-editing methods to elucidate the mechanism of a *Salmonella* deglycase. *J. Mol. Biol.* **431**, 4497–4513.
  - Chan, D.S., Mendes, V., Thomas, S.E., McConnell, B.N., Matak-Vinković, D., Coyne, A.G., et al., (2017). Fragment screening against the EthR-DNA interaction by native mass spectrometry. *Angew. Chem. Int. Ed. Engl.* **56**, 7488–7491.
  - Marty, M.T., Baldwin, A.J., Marklund, E.G., Hochberg, G. K., Benesch, J.L., Robinson, C.V., (2015). Bayesian deconvolution of mass and ion mobility spectra: from binary interactions to polydisperse ensembles. *Anal. Chem.* **87**, 4370–4376.
  - Vigouroux, A., Meyer, T., Naretto, A., Legrand, P., Aumont-Nicaise, M., Di Cicco, A., et al., (2021). Characterization of the first tetrameric transcription factor of the GntR superfamily with allosteric regulation from the bacterial pathogen *Agrobacterium fabrum*. *Nucleic Acids Res.* **49**, 529–546.
  - Rigali, S., Nothhaft, H., Noens, E.E., Schlicht, M., Colson, S., Muller, M., et al., (2006). The sugar phosphotransferase system of *Streptomyces coelicolor* is regulated by the GntR-family regulator DasR and links N-acetylglucosamine metabolism to the control of development. *Mol. Microbiol.* **61**, 1237–1251.